


ORIGINAL ARTICLE

SLC12A5 interacts and enhances SOX18 activity to promote bladder urothelial carcinoma progression via upregulating MMP7

Long Wang¹ | Qun Zhang² | Pei Wu³ | Wei Xiang¹ | Dan Xie⁴ | Ning Wang⁵ | Minhua Deng⁵ | Ke Cao⁶ | Hongliang Zeng⁷ | Zhenzhou Xu⁸ | Xiaoming Liu⁹ | Leye He¹ | Zhi Long¹ | Jing Tan¹ | Jinrong Wang¹ | Bin Liu¹ | Jianye Liu¹ 

¹Department of Urology, The Third Xiangya Hospital of Central South University, Changsha, China

²Department of Radiotherapy, The First Affiliated Hospital of Sun Yat-sen University, Guangzhou, China

³Department of Operation Center, The Second Xiangya Hospital of Central South University, Changsha, China

⁴Department of Pathology, Sun Yat-sen University Cancer Center, Guangzhou, China

⁵Department of Urology, Sun Yat-sen University Cancer Center, Guangzhou, China

⁶Department of Oncology, The Third Xiangya Hospital of Central South University, Changsha, China

⁷Research Institute of Chinese Medicine, Hunan Academy of Chinese Medicine, Changsha, China

⁸Department of Urology, Hunan Cancer Hospital, Changsha, China

⁹Department of Digestive, The Third Xiangya Hospital of Central South University, Changsha, China

Correspondence

Jianye Liu, Department of Urology, The Third Xiangya Hospital of Central South University, No. 138, Tongzipo Road, Changsha, 410013, Hunan Province, China. Email: liujianye810@163.com

Funding information

National Natural Science Foundation of China, Grant/Award Number: 81802556; Scientific Projects of Health Commission of Hunan Province, Grant/Award Number: B2017034; Huxiang Young Talents Plan Project of Hunan Province, Grant/Award Number: 2019RS2015; Hunan Province Natural Science Foundation, Grant/Award Number: 2019JJ30039; Scientific Projects of Changsha Administration of Science & Technology, Grant/Award Number: kq1901129; New Xiangya Talent Projects of the Third Xiangya Hospital of Central South University, Grant/Award Number: JY201615

Abstract

Solute carrier family 12 member 5 (SLC12A5) has an oncogenic role in bladder urothelial carcinoma. The present study aimed to characterize the molecular mechanisms of SLC12A5 in bladder urothelial carcinoma pathogenesis. Functional assays identified that in bladder urothelial carcinoma SLC12A5 interacts with and stabilizes SOX18, and then upregulates matrix metalloproteinase 7 (MMP7). In vivo and in vitro assays were performed to confirm the effect of SLC12A5's interaction with SOX18 on MMP7-mediated bladder urothelial carcinoma progression. SLC12A5 was upregulated in human bladder tumors, and correlated with the poor survival of patients with bladder urothelial carcinoma tumor invasion and metastasis, promoted by SLC12A5 overexpression. We demonstrated that SLC12A5 interacted with SOX18, and then upregulated MMP7, thus enhancing tumor progression. Importantly, SLC12A5 expression correlated positively with SOX18 and MMP7 expression in bladder urothelial carcinoma. Furthermore, SLC12A5 expression was suppressed by miR-133a-3p. Ectopic expression of SLC12A5 partly abolished miR-133a-3p-mediated suppression

Abbreviations: BUC, bladder urothelial carcinoma; CHX, cycloheximide; Co-IP, co-immunoprecipitation; DAPI, 2-(4-aminophenyl)-1H-indole-6-carboxamide; EGFR, epidermal growth factor receptor; HMG, high mobility group; IHC, immunohistochemistry; miRNA, microRNA; OS, overall survival; PBST, PBS-Tween 20; qRT-PCR, quantitative RT-PCR; RC, radical cystectomy; SLC12A5, solute carrier family 12 member 5; SOX18, SRY-box transcription factor 18.

Long Wang, Qun Zhang, and Pei Wu contributed equally to this work.

This is an open access article under the terms of the Creative Commons Attribution-NonCommercial License, which permits use, distribution and reproduction in any medium, provided the original work is properly cited and is not used for commercial purposes.

© 2020 The Authors. *Cancer Science* published by John Wiley & Sons Australia, Ltd on behalf of Japanese Cancer Association.

of cell migration. SLC12A5-SOX18 complex-mediated upregulation on MMP7 was important in bladder urothelial carcinoma progression. The miR-133a-3p/SLC12A5/SOX18/MMP7 signaling axis was critical for progression, and provided an effective therapeutic approach against bladder urothelial carcinoma.

KEYWORDS

bladder urothelial carcinoma progression, miR-133a-3p, MMP-7, SLC12A5, SOX18

1 | INTRODUCTION

BUC ranks ninth among the most commonly diagnosed malignancies and is the 13th highest cause of cancer-related death across the world.¹ In the clinical management of BUC,^{2,3} its etiology, and biomarkers for diagnosis, prognosis, or prediction are well known.^{4,5} Superficial and invasive BUC have available treatment options, however there are limited therapeutic options for metastatic disease, thus it remains a serious clinical challenge. To date, patients with BUC with tumor metastasis have had no available and effective therapies. Therefore, to develop more efficient anticancer treatments, the molecular mechanisms underlying the progression and metastasis in BUC should be determined.

SLC12A5 gene, also known as *KCC2*, is located on chromosome 20q13, which among human cancers is one of the most frequently amplified regions.⁶ SLC12A5 (originally known as an integral membrane KCl cotransporter) was reported to maintain chloride homeostasis in neurons. However, recent studies have shown that mutation and abnormal expression of SLC12A5 is involved in the tumorigenesis and progression of some human cancers.⁷⁻¹² Recently, we found that high expression of SLC12A5 is an independent molecular marker for shortened survival of patients with BUC. Furthermore, downregulation of the SLC12A5 gene, combined with cDNA gene chip analysis, confirmed that matrix metalloproteinase 7 (*MMP7*) is the major downstream target gene of SLC12A5 during induction of BUC invasiveness and metastasis.¹³ SLC12A5's tumor-specific regulation and its downstream targets should be determined, as this would reveal their potentially important clinical applications. Consequently, the aim of the present study was to investigate the oncogenic role of SLC12A5 and its molecular mechanisms in BUC.

In this study, we evaluated expression status of SLC12A5 in a series of primary BUCs from RC specimens and its clinical significance. We also demonstrated that SOX18 is a novel binding partner for SLC12A5. SOX18 interacts with SLC12A5 in vitro and in vivo. Moreover, we provide evidence that SLC12A5 interacts with SOX18, and then upregulates downstream *MMP7* expression to promote BUC cell progression and metastasis. Our findings suggest that SLC12A5 is an oncogene and may be a prognostic factor in BUC that exerts its function by upregulating *MMP7* via SOX18.

2 | MATERIALS AND METHODS

2.1 | Cell lines and clinical samples

The American Type Culture Collection (ATCC) provided 7 human BUC cell lines (UM-UC3, T24, J82, 5637, RT4, EJ, BIU87), and SV-HUV-1, a normal bladder uroepithelial cell line. These cell lines were grown in DMEM (Invitrogen) containing 10% fetal bovine serum. For IHC analysis, as a learning cohort, 112 patients with BUC treated with RC were selected from the Third Xiangya Hospital of Central South University and the Affiliated Cancer Hospital of Xiangya School of Medicine, Central South University. The validation cohort comprised 126 patients with BUC who had been treated with RC at other institutes, including the Cancer Center and the First Affiliated Hospital, Sun Yat-Sen University. The patients were selected based on previously described criteria.^{14,15} Table 1 describes the clinicopathological characteristics of these patients. In addition, between 2015 and 2017, the Third Xiangya Hospital of Central South University provided a panel of 20 fresh BUC tissues and matched adjacent nontumor bladder tissues, which were stored in liquid nitrogen until needed. The Ethical Committee of the Third Xiangya Hospital of Central South University (Changsha, China) approved this study.

2.2 | Stable cell line construction

Vectors pMSCV/SLC12A5 and pMSC/SOX18, which overexpress human SLC12A5 and SOX18, respectively, were constructed by subcloning the PCR-amplified human SLC12A5 and SOX18 coding sequences into vector pMSCV (Clontech). Construction of the SLC12A5 short hairpin RNA (shRNA) lentiviral expression vector has been described previously.¹³ shRNA oligonucleotides (ShRNA: AGAGTTGCCAGGGTTACATTT) were cloned into vector pSuper-retro-puro resulting in pSuper-retro-SOX18-ShRNA. To obtain the recombinant lentiviruses, these vectors were then packaged into 293T cells. The recombinant lentiviruses were then used to produce stable overexpression or knockdown cell lines from BUC cells, as described previously.^{15,16}

For ectopic expression of miR-133a-3p (MIMAT0000427), the primary-miRNA sequence of miR-133a-3p was synthesized (5'-CCGGACAATGCTTTGCTAGAGCTGGTAAAATGGAACCAATCGCCTCTTCAATGGATTTGGTCCCCTTCAACCA

TABLE 1 Clinicopathological correlation of SLC12A5 expression in BUC

Variable	Learning cohort				Validation cohort			
	Cases	Low (%)	High (%)	P ^a	Cases	Low (%)	High (%)	P ^a
Age (y)								
≤66 ^b	56	25 (44.6)	31 (55.4)	.57	72	34 (47.2)	38 (52.8)	.918
>66	56	28 (50.0)	28 (50.0)		54	26 (48.1)	28 (51.9)	
Gender								
Male	90	44 (49.4)	45 (50.6)	.473	114	50 (43.9)	64 (56.1)	.009
Female	22	9 (40.9)	13 (59.1)		12	10 (83.3)	2 (16.7)	
Smoking history								
No	47	27 (57.4)	20 (42.6)	.068	52	26 (50.0)	26 (50.0)	.654
Yes	65	26 (40.0)	39 (60.0)		74	34 (45.9)	40 (54.1)	
Tumor size (cm)								
≤3.6 ^c	58	31 (53.4)	27 (46.6)	.178	71	29 (40.8)	42 (59.2)	.084
>3.6	54	22 (40.7)	32 (59.3)		55	31 (56.4)	24 (43.6)	
Tumor multiplicity								
Unifocal	35	13 (37.1)	22 (62.9)	.146	49	18 (36.7)	31 (63.3)	.051
Multifocal	77	40 (51.9)	37 (48.1)		77	42 (54.5)	35 (45.5)	
Tumor grade								
G1	17	13 (76.5)	4 (23.5)	.016	24	20 (83.3)	4 (16.7)	<.001
G2	43	21 (48.8)	22 (51.2)		46	19 (41.3)	27 (58.7)	
G3	52	39 (36.5)	34 (63.5)		56	21 (37.5)	35 (62.5)	
pT status								
pTa/pT1	31	26 (83.9)	5 (16.1)	<.001	25	17 (68.0)	8 (32.0)	.009
pT2	34	19 (55.9)	15 (44.1)		55	29 (52.7)	26 (47.3)	
pT3	40	6 (15.0)	34 (85.0)		30	11 (36.7)	19 (63.3)	
pT4	7	2 (28.6)	5 (71.4)		16	3 (18.8)	13 (52.4)	
pN status								
pN-	86	47 (54.7)	39 (45.3)	.005	105	57 (54.3)	48 (45.7)	.001
pN+	26	6 (23.1)	20 (76.9)		21	3 (14.3)	18 (85.7)	
Adjuvant chemotherapy								
No	71	47 (66.2)	24 (33.8)	<.001	93	54 (57.0)	39 (43.0)	<.001
Yes	41	6 (14.6)	35 (85.4)		33	6 (15.2)	27 (84.8)	

Abbreviation: BUC, bladder urothelial carcinoma.

^aChi-square test.

^bMedian age.

^cMedian size.

GCTGTAGCTATGCATTGATTTTTGAATTC-3'), and then ligated into the human RNA interference consortium vector pLKO.1 via its *Age*1 and *Eco*R1 sites. To knockdown miR-133a-3p expression, we designed a miR-133a-3p inhibitor (inhibitor-miR-133a-3p) (Ribobio) together with the appropriate control (inhibitor-Ctrl). The inhibitor and plasmid constructs were transfected into cells using Lipofectamine 3000 (Invitrogen). In summary, the p3000 fraction and plasmids were mixed at a certain ratio, and then added to the cells. Inhibitors and mimics were incubated directly with the Lipofectamine 3000 fraction and added to the cells according to the manufacturer's protocol.

2.3 | qRT-PCR

Total RNA from BUC tissues and cell lines was extracted using TRIzol reagent (Invitrogen). SYBR Green SuperMix (Roche Molecular Systems Inc) was used to carry out qRT-PCR together with an ABI7900HT Fast Real-Time PCR system (Applied Biosystems). GAPDH (encoding glyceraldehyde-3-phosphate dehydrogenase) was used as the internal control. PCR primer sequences were: SLC12A5, forward: 5'-GCAGGAGCCATGTACATCCT-3' and reverse: 5'-CCATGCAGGTGAGCACACA-3'; SOX18, forward: 5'-TT CGACCAGTACCTCAACTGC-3' and reverse: 5'-GACATGGAACCAA

ACATACACG-3'; MMP7, forward: 5'-CAGGAAGCCGAGAAGTGAC-3' and reverse: 5'-TCTCCGGCAAACCGAAGAAC-3'; GAPDH, forward: 5'-GGAGATTGTTGCCATCAACG-3' and reverse: 5'-TTGGTGGTGCAGGATGCATT-3'. Relative expression levels of MMP7, SOX18, and SLC12A5 are shown as $-\Delta C_T$ (cycle threshold) values.

2.4 | Western blotting and drug administration

Cells were lysed using lysis buffer to obtain total proteins, which were separated using 12% sodium dodecyl sulfate polyacrylamide gel electrophoresis and then transferred onto polyvinylidene fluoride (PVDF) membranes (Millipore). PVDF membranes were blocked for 1 h, then the membranes were incubated with monoclonal antibodies overnight at 4°C. Secondary antibodies were then reacted with the membranes for 1 h at room temperature. Enhanced chemiluminescence (ECL kit, Santa Cruz Biotechnology Inc) was used to visualize the immunoreactive protein bands and the band intensities were analyzed using the Quantity One system (Bio-Rad). Primary antibodies comprised: anti-SLC12A5 (1:1000 dilution, Abcam), anti-SOX18 (1:1000 dilution, Cell Signaling Technology), anti-MMP7 (1:1000 dilution, Abcam), anti-MMP2 (1:800 dilution, Abcam), anti-MMP9 (1:1000 dilution, Abcam), and anti-GAPDH (1:5000 dilution, Cell Signaling Technology). For western blotting experiments, CHX was used at 100 µg/mL for 24 h (Sigma-Aldrich).

2.5 | IHC staining

After staining with primary antibodies, a Dako Real Envision Kit (Dako) was used to visualize protein expression, according to the manufacturer's instructions. Two independent experienced pathologists scored the staining intensity manually. To evaluate IHC staining, previously published scoring criteria for SLC12A5,¹³ SOX18,¹⁷ or MMP7¹³ were used. Primary antibodies comprised: anti-SLC12A5 (1:100 dilution, Abcam), anti-SOX18 (1:200 dilution, Cell Signaling Technology), and anti-MMP7 (1:1000 dilution, Abcam).

2.6 | Immunofluorescence

BUC cells were grown on confocal dishes (Corning Inc), rinsed twice with PBS and then fixed for 15 min using 4% paraformaldehyde in PBS on ice. Cells were washed 3 times with PBS, and then permeabilized using 0.1% Triton X-100 in PBS on ice for 10 min. After washing twice with PBS, they were blocked using 5% BSA in PBST at 37°C for 30 min. Cells were then incubated with primary antibodies at 37°C for 1 h. Cells were washed with PBST, then cells were incubated with the corresponding secondary antibodies for 30 min at 37°C. The cells were then stained with DAPI to stain the nuclei. Fluorescent images were acquired using an OLYMPUS FV1000 confocal microscope (Olympus). Relative mean

fluorescence densities were analyzed using ImageJ software (NIH) and plots were constructed using GraphPad Prism 6 software (GraphPad Software, Inc).

2.7 | Co-IP

Cell extracts were incubated with protein A-agarose and antibodies (Pierce Biotechnology) overnight at 4°C. Negative controls comprised normal mouse or rabbit IgG (Santa Cruz Biotechnology). Proteins were washed 5 times using lysis buffer (radioimmunoprecipitation assay (RIPA) buffer; Beyotime, Jiangsu, China; P0013), and then 2× SDS sample buffer was used to elute the proteins bound to the beads by boiling for 8 min at 100°C. Western blotting was then used to analyze the samples.

2.8 | GST-pull-down

Reverse transcription PCR was used to isolate the SLC12A5 cDNA, which was cloned into GST-tagged pGEX-4T-1 vector via the XhoI and EcoRI sites using T4 DNA Ligase (Thermo Scientific). SOX18 cDNA was also cloned into the XhoI and EcoRI sites of the His-tagged pET-28a(+) vector. Recombinant plasmids pET-28a(+)-SOX18p and GEX-4T-1-SLC12A5 were transformed separately into *Escherichia coli* BL21(DE3). Screening and identification of positive clones synthesizing high levels of recombinant GST-SLC12A5 or His-SOX18 proteins were assessed using double enzyme digestion, PCR identification, and DNA sequencing. Purified GST-SLC12A5 fusion proteins were then linked to Glutathione Sepharose (GE Healthcare), mixed, and reacted with purified His-SOX18 at 4°C overnight. Western blotting analysis using anti-GST antibodies (TransGen Biotechnology) and anti-His tag antibodies (Beijing, China) was used to detect the proteins in the eluted samples.

2.9 | Chromatin immunoprecipitation (ChIP) assay

ChIP assay was conducted using an EZ ChIP™ Chromatin Immunoprecipitation Kit (Millipore). In summary, sonication was used to break the crosslinked chromatin into 200-1000 bp fragments. Anti-SOX18 (1:200 dilution, Cell Signaling Technology) and anti-MMP7 (1:1000 dilution, Abcam) antibodies were then used to immunoprecipitate the chromatin.

2.10 | 3-(4,5-Dimethylthiazol-2-yl)-2,5-diphenyltetrazolium bromide (MTT) assay

Cell viability was measured using an MTT assay (Sigma-Aldrich). Briefly, seeded cells were cultured in 96-well plates. The manufacturer's procedures for the MTT assay were then followed to examine cell viability.

2.11 | Transwell assays

After resuspension in 200 μ l serum-free medium, 3.0×10^4 BUC cells were added to the upper section of a Transwell chamber (Corning; 24-well insert, pore size: 8 mm). Fetal bovine serum (15%) was added to the lower section as a chemoattractant. For the migration assay, the Transwell apparatus was incubated for 48 h. Thereafter, adherent cells on the upper surface of the membrane were discarded, and those on the lower surface were fixed, followed by staining with 0.1% crystal violet. For each insert, cells were counted visually in 5 randomly chosen fields under a light microscope.

2.12 | Luciferase reporter assay

A psiCHECK-2-SLC12A5-3'-UTR reporter and the miR-133a-3p mimics or negative control, were co-transfected into BUC cells. At 36 h later, a Dual-Luciferase Reporter Assay System (Promega) was then used to analyze the collected cells.

Next 100 ng of the SOX18 luciferase reporter plasmid or the control-luciferase plasmid, together with 1 ng of the pRL-TK Renilla plasmid (Promega), were transfected into cells using Lipofectamine 3000, according to the manufacturer's instructions. Then, 24 h later, the Renilla and Luciferase signals were detected using the Dual-Luciferase Reporter Assay Kit (Promega).

2.13 | Care and maintenance of the experimental animals

All procedures involving mice were approved by the Institutional Animal Care and Use Committee of the Third Xiangya Hospital of Central South University. Intravenous injection of 5×10^5 BUC cells into the tail vein of 4-wk-old BALB/c nude mice was used to establish the in vivo metastasis model. The mice were sacrificed at 6 wk after injection. Lungs were excised before being fixed using phosphate-buffered formalin. Subsequently, for each block of the lung, consecutive tissue sections were obtained. We carefully enumerated the pulmonary metastatic nodules in the lungs.

2.14 | Statistical analysis

In the BUC cohorts, SPSS software (SPSS Standard version 16.0; IBM Corp.) was used to carry out the statistical analysis. Statistical significance of the association of SLC12A5 expression with the patients' clinicopathological parameters and their correlations were assessed using the χ^2 test. Primary end points were OS. OS was assessed via Kaplan-Meier analysis, and comparisons of OS data were performed using the log-rank test. For multivariate analysis, the Cox regression model was used. Mean \pm SD was used to express all the

data. To assess differences within treatment groups Dunnett *t* test and two-factor analysis of variance were used. Statistical significance was accepted at $P < .05$.

3 | RESULTS

3.1 | Expression of SLC12A5 in BUC

SLC12A5 expression in patients with BUC was studied by recruiting 2 independent BUC cohorts, in which 112 and 126 BUC tissue samples were collected, respectively. The clinicopathological characteristics of the patients studied are summarized in Table 1. Using previously reported criteria, 59/112 (52.7%) BUC patients in the learning cohort and in 66/126 (52.4%) BUC patients in the validation cohort showed high SLC12A5 expression (Figure 1A-D). In both the learning and validation cohorts, correlation analysis demonstrated that high SLC12A5 expression was associated significantly with higher grade, advanced T and N status, and adjuvant chemotherapy ($P < .05$; Table 1).

3.2 | Expression of SLC12A5 predicts poor OS for patients with BUC

In the learning and validation cohorts, univariate analysis showed that poor OS for patients with BUC correlated with high SLC12A5 expression ($P < .001$ and $P = .002$, respectively; Figure 1E,F; Table S1). In both cohorts, Kaplan-Meier analysis also revealed a significant effect of number of clinicopathological prognostic parameters, including pT status ($P = .009$ and $P < .001$, respectively; Table S1), pN status ($P < .001$ and $P < .001$, respectively; Table S1), and adjuvant chemotherapy ($P < .001$ and $P < .001$, respectively; Table S1) on OS. In the learning cohort, multivariate analysis demonstrated that pN status and SLC12A5 expression were independent predictors of patient OS ($P = .001$ and $P < .001$, respectively; Table 2). This result was verified in the validation cohort ($P = .019$ and $P = .026$, respectively; Table 2).

3.3 | In vitro and in vivo BUC cell invasion and migration are promoted by SLC12A5 overexpression

To study the function of SLC12A5 in BUC cells, SLC12A5 expression in one normal bladder uroepithelial cell line (SV-HUV-1) and 7 BUC cell lines was examined. qRT-PCR and western blotting assays showed higher expression of SLC12A5 in 4 BUC cell lines (EJ, T24, BIU87, and RT4) and lower SLC12A5 levels in 3 BUC cell cells (J82, 5637, and UM-UC-3) and in the normal SV-HUV-1 cells (Figure 2A,B). Previously, we reported that BUC cell invasion and metastasis was inhibited by downregulation of SLC12A5 in vitro and in vivo.¹³ Next, we studied the effect of SLC12A5 overexpression on in vitro and in vivo BUC cell invasion and metastasis.

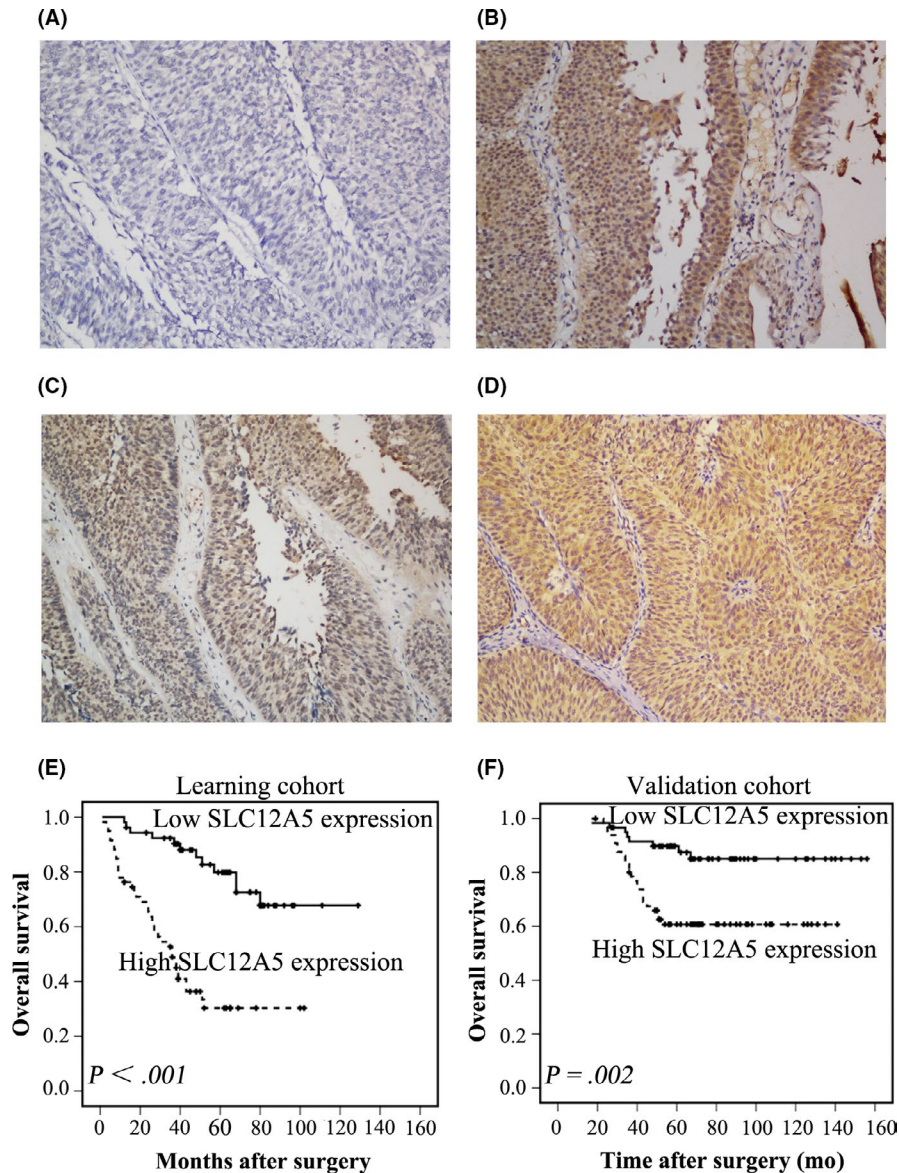


FIGURE 1 Immunohistochemical staining of SLC12A5 in BUC tissues and its prognostic significance in patients with BUC. A, BUC case (case 6) exhibiting low expression of SLC12A5, in which less than 20% of carcinoma cells showed positive staining for SLC12A5. B-D, High expression of SLC12A5 was observed in other BUC (cases 21, 45, 78), in which more than 80% of carcinoma cells demonstrated positive staining for SLC12A5. E, F High expression of SLC12A5 was associated with poor prognosis of patients with BUC. Kaplan-Meier plots show the overall survival curves of 112 patients with BUC in the learning cohort (E) and 126 patients with BUC in the validation cohort (F), according to SLC12A5 expression levels in the primary tumor ($P < .05$, log-rank test)

Feature	Learning cohort			Learning cohort		
	HR	95%CI	P	HR	95%CI	P
pT status (pTa/pT1 vs pT2 vs pT3 vs pT4)	0.759	0.667-1.344	.947	1.626	0.959-2.756	.071
pN status (pN- vs pN+)	2.132	1.023-4.446	.043	2.653	1.070-6.580	.035
Adjuvant chemotherapy (no vs yes)	2.045	0.889-4.704	.092	1.188	0.376-3.755	.769
SLC12A5 expression (low vs high)	3.623	1.707-7.689	.001	1.997	0.967-4.124	.041

Abbreviations: BUC, bladder urothelial carcinoma; CI, confidence interval; HR, hazard ratio.

TABLE 2 Multivariate Cox regression analysis for overall survival in BUC patients

SLC12A5 was overexpressed in 5637 and UM-UC-3 cell lines (Figure 2C,D). A proliferation assay revealed that SLC12A5 overexpression had no effect on the growth of UM-UC-3 and 5637 cells (Figure S1A,B). However, Boyden chamber assays demonstrated that SLC12A5 increased the migration of 5637 and UM-UC-3 cells

across the Transwell membrane by 3-fold to 4-fold (Figure 2E). Similarly, the numbers of 5637 and UM-UC-3 cells that invaded through Matrigel in the Transwell insert were also significantly increased by SLC12A5 overexpression (Figure 2F). Next, we studied the effect of SLC12A5 overexpression on BUC metastasis to the

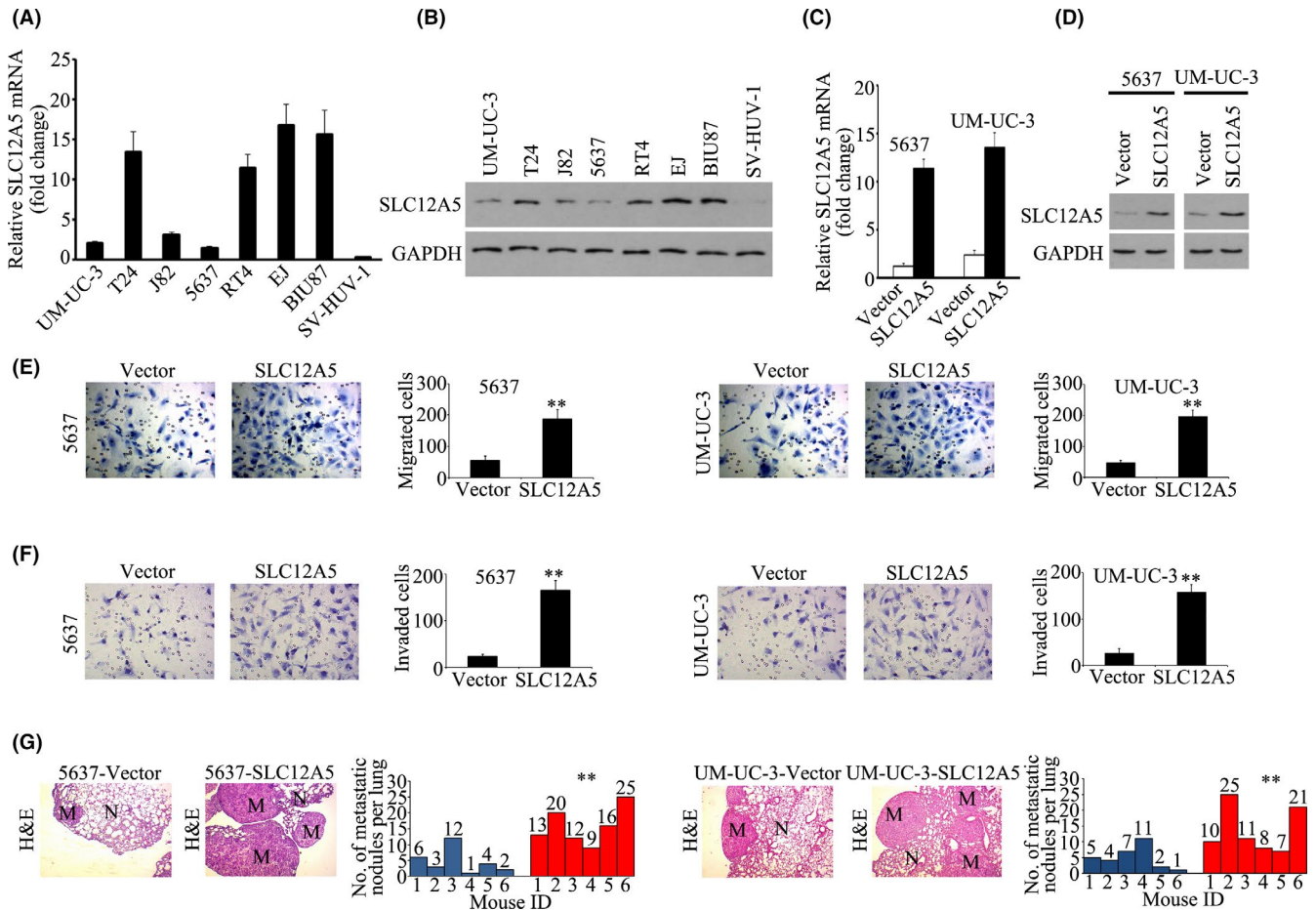


FIGURE 2 Overexpression of SLC12A5 promotes BUC invasion and metastasis in vitro and in vivo. A, B, qRT-PCR and western blotting showing the relative expression of SLC12A5 mRNA (A) and protein (B) in several BUC cell lines and normal bladder uroepithelial cell line SV-HUV-1. C, D, qRT-PCR and western blotting showing the relative expression of SLC12A5 mRNA (C) and protein (D) after overexpressing SLC12A5 in 5637 and UM-UC-3 cell lines. E, F, Transwell migration assays showing that overexpression of SLC12A5 promoted the migration (E) and invasion (F) of 5637 and UM-UC-3 cell lines. G, Tail vein injection lung metastatic models. Number of tumors was compared between the SLC12A5-vector group and the SLC12A5-overexpressing group. $n = 6$. N, normal lung; M, lung metastatic tumor; $**P < .01$

lungs after intravenous tail vein delivery of BUC cells. In the lungs of mice, H&E staining revealed that the metastatic burden was significantly increased 6 wk after injection of 5637 and UM-UC-3 cells overexpressing SLC12A5 (Figure 2G). These data indicated that overexpression of SLC12A5 promoted BUC cells invasiveness and metastasis in vitro and in vivo.

3.4 | SLC12A5 interacts with SOX18 in BUC cells

Previously, we used gene chip technology to confirm that *MMP7* is the major downstream target gene of SLC12A5 during the induction of BUC invasiveness and metastasis.¹³ SOX18, one of the 20-member SOX transcription factor family, shares the characteristic HMG box.¹⁸ SOX18 determines cell fate and regulates cell differentiation during embryonic development.^{18,19} Previous studies have found that SOX18 is upregulated and enhances cell proliferation and metastasis in various human malignancies, including breast,

lung, ovarian, hepatocellular, and bladder cancer.^{17,20-23} The master transcription factor SOX18 has been identified on the promoter of *MMP7*.²⁴ Thus, we determined whether SLC12A5 physically interacts with SOX18. In BUC cells, the expression level of SOX18 mRNA was unaffected by SLC12A5 overexpression (Figure 3A); however, in 5637 and UM-UC-3 cells, overexpression of SLC12A5 increased the SOX18 protein level; in T24 cells, SLC12A5 knock-down had the opposite effect (Figure 3B). Thus, SLC12A5 functions to increase the SOX18 protein level. To further investigate SOX18 control mediated by SLC12A5, the interaction of these 2 proteins was examined. A significant amount of SLC12A5 protein was associated with SOX18 in the Co-IP assay (Figure 3C). In 5637 and UM-UC-3 cells, confocal microscopy revealed the co-localization of SOX18 and SLC12A5 (Figure 3D). To determine whether there is a direct interaction between these 2 proteins, GST-pull-down assays were performed using purified His-tagged SOX18 and GST-tagged SLC12A5. The results shown in Figure 3E revealed that purified His-tagged SOX18 associated with GST-SLC12A5, but not with

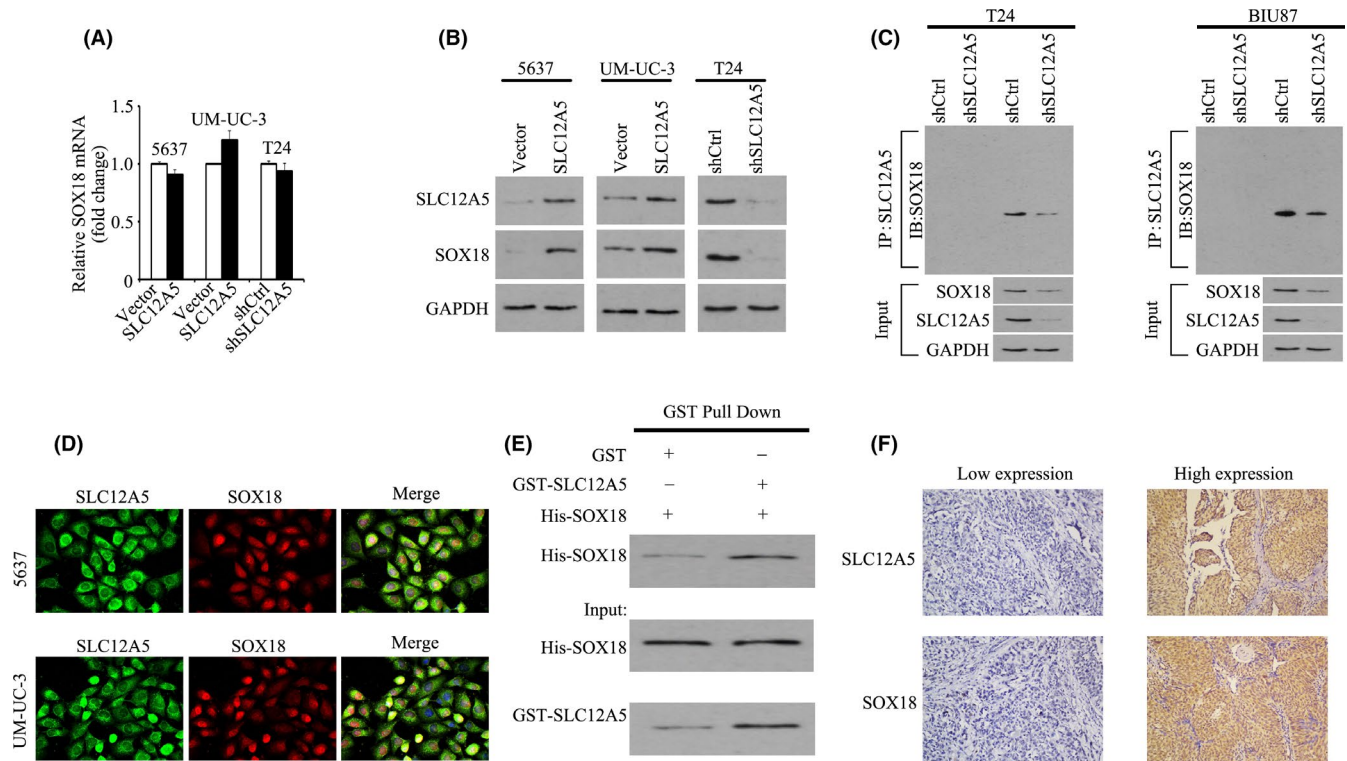


FIGURE 3 SLC12A5 interacts with SOX18. A, BUC cells were transfected with the SLC12A5 overexpression or knockdown vector. SOX18 mRNA level was determined. B, Protein level of SOX18 was examined in cells with SLC12A5 overexpression or knockdown. C, Co-immunoprecipitation assays of SLC12A5 and SOX18 in T24 and BIU87 cells. T24 and BIU87 cells were transfected with nontargeting shRNA or SLC12A5 shRNA. Cell lysates were immunoprecipitated with IgG control antibodies or anti-SOX18 antibodies, and then immunoblotted with anti-SLC12A5 or anti-SOX18 antibodies. SLC12A5, SOX18, and GAPDH levels in whole cell lysates (input) are shown. D, BUC cells were fixed in 4% paraformaldehyde and incubated with antibodies overnight at 4°C. Cells were stained with fluorescent secondary antibodies and DAPI, then cells were observed under a confocal fluorescence microscope. E, Purified bacterially expressed His-SOX18 fusion proteins were mixed with purified bacterially expressed GST or GST-SLC12A5 fusion proteins. Immunoprecipitated His-tagged fusion proteins were detected using western blotting analysis with anti-His antibodies. Lower panels show the inputs of His-SOX18 and GST-SLC12A5 fusion proteins in the immunoprecipitation experiment. F, Patients with high expression of the SLC12A5 in BUC tissues frequently showed high expression of SOX18

GST (Figure 3E). Moreover, patients with BUC with high SLC12A5 levels frequently showed high expression of SOX18 (Figure 3F; Table S2). The correlation between SOX18 expression in BUC and several clinicopathologic features was further studied. In the learning cohort, SOX18 expression was positively correlated with smoking history, tumor size, tumor multiplicity, T and N status, and adjuvant chemotherapy ($P < .05$; Table S3); In the validation cohort, SOX18 expression was positively correlated with gender, tumor size, tumor multiplicity, tumor grade, T and N status, and adjuvant chemotherapy ($P < .05$, Table S3). Importantly, high expression of SOX18 was associated with poor OS in these 2 cohorts ($P < .001$ and $P = .007$, respectively; Figure S2). Short hairpin RNA (shRNA) was used to knockdown SLC12A5 expression to determine whether SLC12A5 modulates SOX18 levels. After 48 and 72 h of shRNA delivery, in SLC12A5-depleted cells, decreased levels of the SOX18 protein were observed, whereas there was no effect on its mRNA level (Figures S3, S4). Inhibition of protein synthesis by CHX for different times, followed by analysis using western blotting, suggested that SOX18 half-life was markedly extended after SLC12A5 knockdown (Figure S5). These data indicated that SLC12A5 directly

physically interacts with SOX18 to regulate SOX18 protein stability, and that their expression levels are correlated in BUC.

3.5 | SLC12A5 activates the SOX18 target gene MMP7 in BUC cells

To determine whether SLC12A5 regulates SOX18's transcriptional activity, we first performed SOX18 luciferase reporter assays. SLC12A5 overexpression enhanced the SOX18 luciferase reporter gene activity significantly. By contrast, SLC12A5 silencing induced a significant decrease in the reporter activity (Figure 4A). ChIP analysis demonstrated that the MMP7 promoter region was enriched with SOX18 (Figure 4B). Moreover, western blotting and qRT-PCR analyses verified that in 5637 and UM-UC-3 cells, SLC12A5 induced transcription of MMP7 (the SOX18 target gene). However, MMP7 expression was significantly attenuated by SLC12A5 knockdown in T24 cells (Figure 4C,D). Additionally, patients with BUC who had high SLC12A5 levels frequently showed high expression of MMP7 (Table S2). Western blotting showed that SLC12A5 overexpression

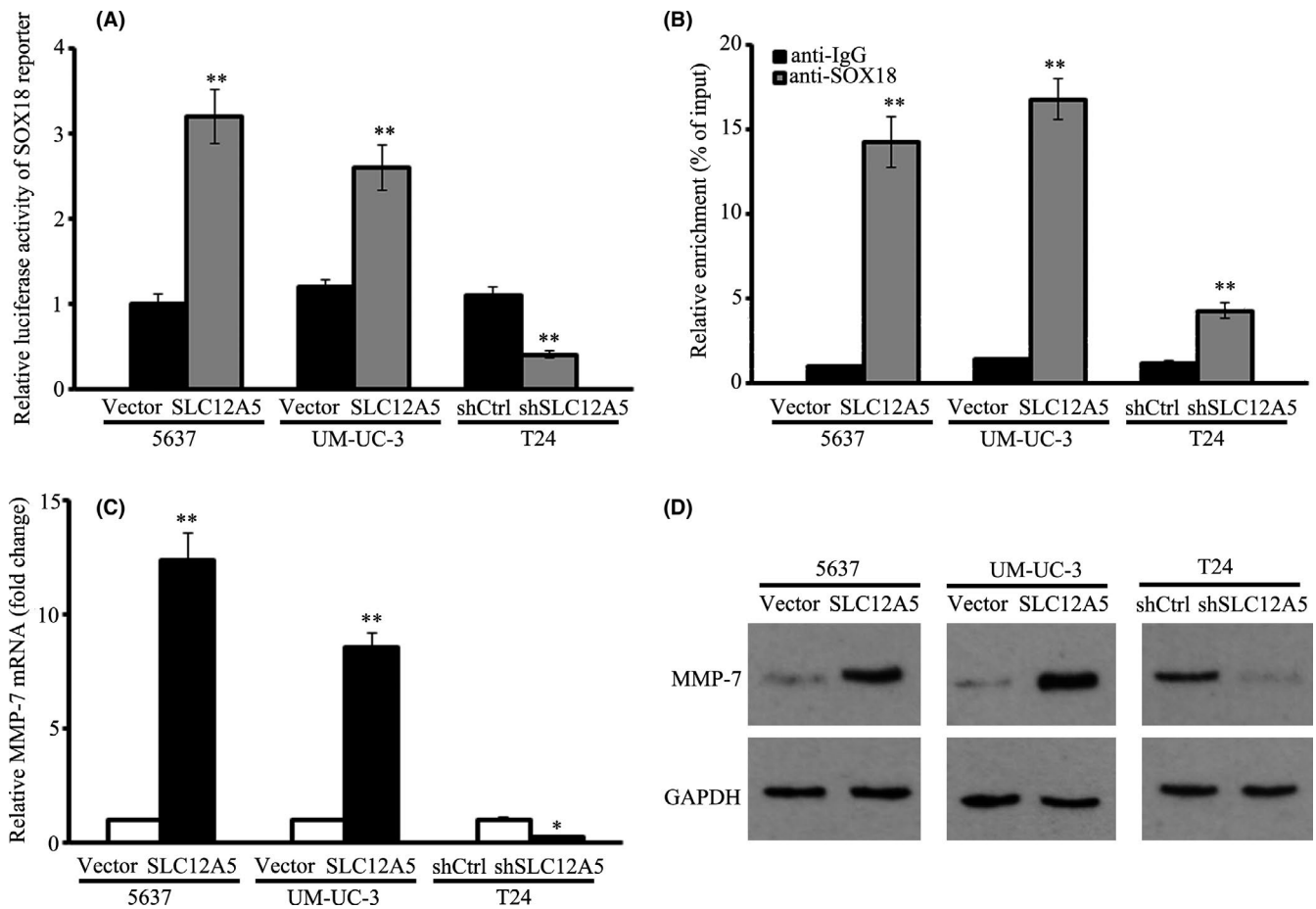


FIGURE 4 SLC12A5 regulates the expression of SOX18 target gene *MMP7* in BUC cells. A, SOX18 luciferase reporter activities were analyzed in the indicated cells. Each bar represents the mean \pm SD of 3 independent experiments. B, ChIP assay using anti-SOX18 antibodies to test the enrichment at the *MMP7* promoter. C, *MMP7* mRNA level was examined in BUC cells with SLC12A5 overexpression or knockdown. D, Protein level of *MMP7* was examined in cells with SLC12A5 overexpression or knockdown; ** $P < .01$

had no effect on the expression of other MMPs, such as *MMP2* and *MMP9* in UM-UC-3 and 5637 cells (Figure S6). These results indicated that SLC12A5 colocalizes with SOX18 and activates its target gene *MMP7* in BUC cells.

3.6 | SOX18 or MMP7 inhibition impairs SLC12A5-induced BUC cell progression

SLC12A5 can enhance SOX18 transactivation ability; therefore, we sought to determine whether SOX18 transactivation is required for SLC12A5-induced BUC cell progression. The results of western blotting demonstrated that SOX18 levels increased in BUC cells after the overexpression of SLC12A5 (Figure S7A). Moreover, in 5637 and UM-UC-3 cells that overexpressed SLC12A5, SOX18 knockdown led to rescued SOX18 levels (Figure S7A). Boyden chamber assays showed that SLC12A5-related enhanced 5637 and UM-UC-3 cell migration and invasion were abolished after treatment with the SOX18 shRNA (Figure S7B,C). In addition, *MMP7* knockdown rescued the ability of SLC12A5 overexpression to promote 5637 and UM-UC-3 cell migration and invasion (Figure S7D,E). Taken together, these findings

indicated that SLC12A5 activates *MMP7* expression by interacting with SOX18, which mediates the migration and invasion of BUC.

3.7 | SLC12A5 is targeted by miR-133a-3p in BUC

starBase prediction program (<http://starbase.sysu.edu.cn/starbase2/index.php>) was used to perform bioinformatic analysis to identify miRNAs that might regulate SLC12A5. This was achieved by comparing the predicted miRNAs with those identified as being downregulated in BUC tumor tissues in previously published miRNA profiles (NCBI/GEO/GSE76211; NCBI/GEO/GSE39093). Screening of the 2 datasets identified only one common miRNA, miR-133a-3p. A putative binding site for miR-133a-3p in the SLC12A5 3' untranslated region (UTR) was identified (Figure 5A). In T24 and 5637 cells, miR-133a-3p overexpression markedly reduced the protein and mRNA levels of SLC12A5 (Figure 5B-D). Whereas downregulation of miR-133a-3p had the opposite effects (Figure 5B-D). The activity of the wild-type 3'UTR of SLC12A5 was attenuated by miR-133a-3p overexpression, but it had no effect on the activity of the mutant 3'UTR, as shown by dual-luciferase reporter assay (Figure 5E). In clinical samples, the

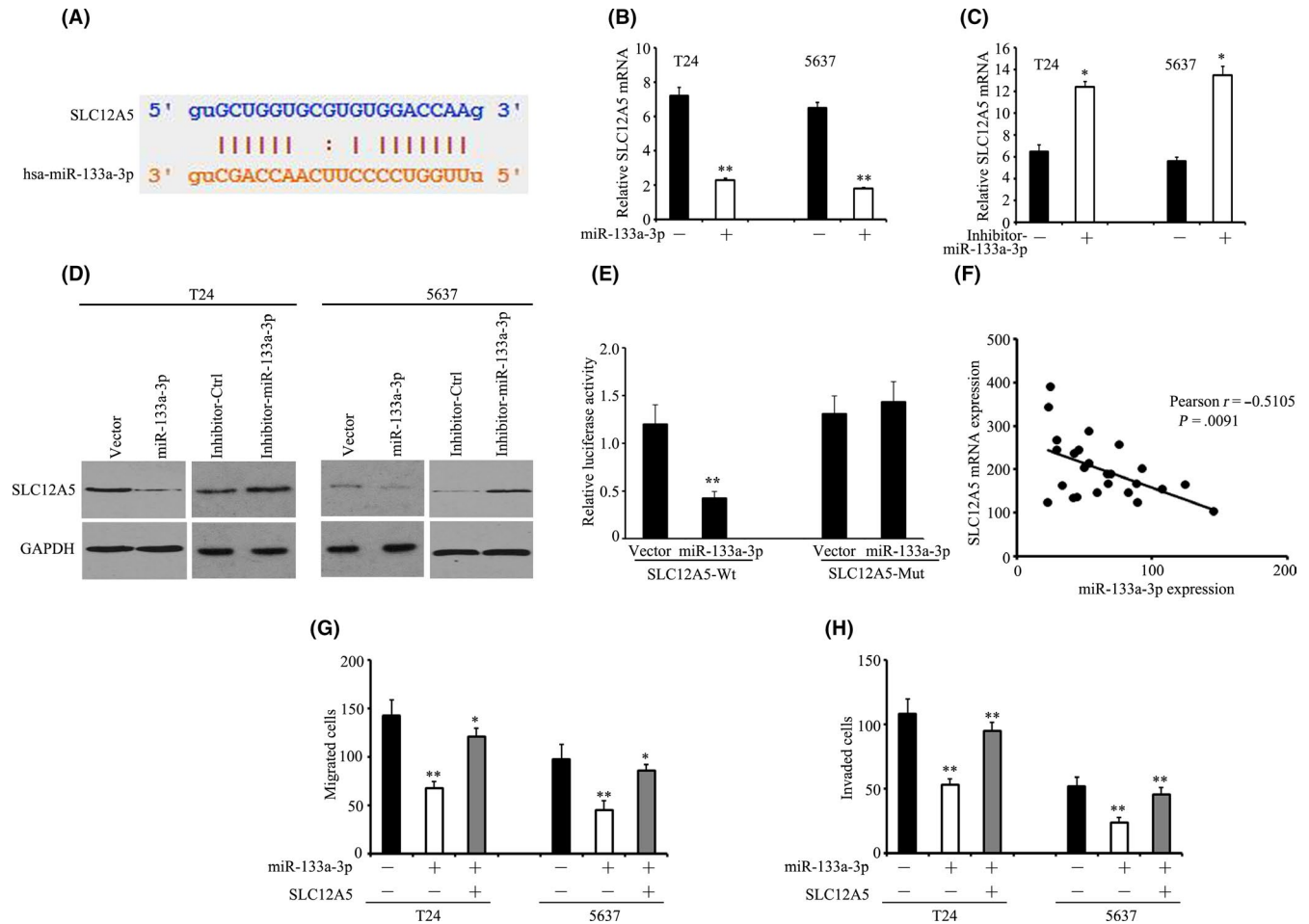


FIGURE 5 SLC12A5 is targeted by miR-133a-3p. A, Putative binding site for miR-133a-3p in the SLC12A5 3'UTR. B, C, T24 and 5637 cells were transfected with miR-133a-3p mimics for 36 h. SLC12A5 mRNA levels were determined using qRT-PCR. D, Proteins from T24 and 5637 cells treated with miR-133a-3p mimics or miR-133a-3p inhibitors were subjected to western blotting to examine the levels of SLC12A5. E, Luciferase reporter assays were performed to indicate the effect of miR-133a-3p on the activity of the SLC12A5 mRNA 3'UTR. F, Correlation between SLC12A5 mRNA and miR-133a-3p was determined in 20 BUC samples. G, H, Impact of SLC12A5 on miR-133a-3p-mediated cell migration was determined by Transwell migration (G) and Matrigel invasion (H) assays; * $P < .05$, ** $P < .01$

SLC12A5 mRNA level was inversely proportional to the expression level of miR-133a-3p (Figure 5F). These results implied that in BUC cells, miR-133a-3p modulates the expression of SLC12A5.

Our results validated previous reports^{25,26} that miR-133a-3p functions as a tumor suppressor in BUC (Figure 5G,H). We then determined the effect of SLC12A5 on miR-133a-3p-induced phenotypes. SLC12A5 overexpression in miR-133a-3p-BUC cells abrogated miR-133a-3p-induced suppression of BUC cell migration and invasion (Figure 5G,H). Additionally, miR-133a-3p decreased SOX18 and MMP7 expression was increased by overexpression of SLC12A5 in T24-miR-133a-3p cells (Figure S8). Taken together, these results implied that SLC12A5 participates in miR-133a-3p's tumor suppressive activity.

4 | DISCUSSION

In this study, we demonstrated frequent upregulation of SLC12A5 in BUC that correlated significantly with malignant phenotypes such

as poorer survival rates and metastasis. SLC12A5 might be an independent prognostic biomarker of poorer outcome in BUC, as demonstrated by multivariate analyses. In accordance with the results reported in our previous study,¹³ our data suggested that SLC12A5 overexpression markedly increased BUC cells' migratory ability through their expression of SOX18, which then transcriptionally activates expression of its downstream target MMP7. These findings identified SLC12A5, SOX18, and MMP7 as potential prognostic markers that might help to guide individual therapeutic management of patients with BUCs.

Although MMPs are the major downstream target genes through which SLC12A5 has been proposed to promote tumor progression and metastasis,¹² the underlying molecular mechanisms remain unclear. In BUC, SLC12A5's oncogenic function promoted tumor progression and metastasis via its expression of SOX18. SOX18 regulates cell differentiation and determines cell fate during embryonic development.^{18,19} Saitoh and colleagues first observed the increased expression of SOX18 in various

cancer cell lines²⁷ and, subsequently, studies have shown that in several types of cancer, such as bladder, lung, pancreatic, and breast cancers, SOX18 is upregulated and is a marker of poor patient prognosis.^{20,22,23,28} Acting as a master transcription factor, SOX18 activates prosurvival signaling pathways, which results in cancer cell migration and proliferation. Moreover, SOX18 could promote prostate cancer growth and metastasis by upregulating MMP7 expression.²⁹ The results of the present study showed that SLC12A5 is physically bound to SOX18, and then transcriptionally activates the expression of the downstream target gene MMP7. Moreover, SLC12A5-promoted cell progression was markedly abolished by inhibition of SOX18 or MMP7. Thus, in BUC, the SLC12A5/SOX18/MMP7 axis could be a therapeutic target.

Dysregulation of microtubule proteins is caused by post-transcriptional modulation of mRNA. As far as we know, there has been no report of SLC12A5 being targeted by miRNAs. Here, miR-133a-3p was identified as an upstream regulator that suppresses SLC12A5 expression in BUC cells. Cell migration could be markedly inhibited by miR-133a-3p overexpression, however this effect was attenuated markedly after SLC12A5 overexpression. The results also indicated that miR-133a-3p caused a reduction in SLC12A5 expression by suppressing SLC12A5 promoter activity. Previous studies have reported the role of miR-133a-3p in BUC.^{25,26,30,31} Their data showed that in BUC, downregulation of miR-133a-3p expression suggested that it acts as a tumor suppressor via its interactions with, for example, the EGFR.³¹

In summary, SLC12A5 promoted *in vitro* BUC cell migration and invasion and metastasis of BUC xenografts in nude mice. SOX18 expression is required for these effects, and the subsequent enhanced expression of MMP7, which contribute to BUC progression. Our data demonstrated that SLC12A5 functions as an oncogene via SOX18-mediated MMP7 expression. In BUC tissues, downregulation of miR-133a-3p results in SLC12A5 upregulation, and poor patient prognosis is associated with SLC12A5 overexpression. The newly identified miR-133a-3p/SLC12A5/SOX18/MMP7 axis might be developed as a therapeutic target to treat BUC.

ACKNOWLEDGMENTS

The study was supported by granted from the National Natural Science Foundation of China (No. 81802556), the Hunan Province Natural Science Foundation (No. 2019JJ30039), Huxiang Young Talents Plan Project of Hunan Province (No. 2019RS2015), the New Xiangya Talent Projects of the Third Xiangya Hospital of Central South University (No. JY201615), the Scientific Projects of Changsha Administration of Science & Technology (No. kq1901129), and the Scientific Projects of Health Commission of Hunan Province (No. B2017034).

DISCLOSURE

The authors declare that they have no conflicts of interest.

ORCID

Jianye Liu  <https://orcid.org/0000-0002-7953-3672>

REFERENCES

1. Antoni S, Ferlay J, Soerjomataram I, et al. Bladder cancer incidence and mortality: a global overview and recent trends. *Eur Urol*. 2017;71:96-108.
2. Abufaraj M, Gust K, Moschini M, et al. Management of muscle invasive, locally advanced and metastatic urothelial carcinoma of the bladder: a literature review with emphasis on the role of surgery. *Transl Androl Urol*. 2016;5:735-744.
3. Hirotsu Y, Yokoyama H, Amemiya K, et al. Genomic profile of urine has high diagnostic sensitivity compared to cytology in non-invasive urothelial bladder cancer. *Cancer Sci*. 2019;110:3235-3243.
4. Sanli O, Dobruch J, Knowles MA, et al. Bladder cancer. *Nat Rev Dis Primers*. 2017;3:17022.
5. Miyake M, Morizawa Y, Hori S, et al. Diagnostic and prognostic role of urinary collagens in primary human bladder cancer. *Cancer Sci*. 2017;108:2221-2228.
6. Tanikawa C, Kamatani Y, Takahashi A, et al. GWAS identifies two novel colorectal cancer loci at 16q24.1 and 20q13.12. *Carcinogenesis*. 2018;39:652-660.
7. Burrell RA, McGranahan N, Bartek J, et al. The causes and consequences of genetic heterogeneity in cancer evolution. *Nature*. 2013;501:338-345.
8. Singh R, Dagar P, Pal S, et al. Significant alterations of the novel 15 gene signature identified from macrophage-tumor interactions in breast cancer. *Biochim Biophys Acta Gen Subj*. 2018;1862:669-683.
9. Wei W-C, Akerman CJ, Newey SE, et al. The potassium-chloride cotransporter 2 promotes cervical cancer cell migration and invasion by an ion transport-independent mechanism. *J Physiol*. 2011;589:5349-5359.
10. Yu C, Yu J, Yao X, et al. Discovery of biclonal origin and a novel oncogene SLC12A5 in colon cancer by single-cell sequencing. *Cell Res*. 2014;24:701-712.
11. Yu J, Wu WKK, Li X, et al. Novel recurrently mutated genes and a prognostic mutation signature in colorectal cancer. *Gut*. 2015;64:636-645.
12. Xu L, Li X, Cai M, et al. Increased expression of Solute carrier family 12 member 5 via gene amplification contributes to tumour progression and metastasis and associates with poor survival in colorectal cancer. *Gut*. 2016;65:635-646.
13. Liu JY, Dai YB, Li X, et al. Solute carrier family 12 member 5 promotes tumor invasion/metastasis of bladder urothelial carcinoma by enhancing NF-kappaB/MMP-7 signaling pathway. *Cell Death Dis*. 2017;8:e2691.
14. Liu J, Li Y, Liao Y, et al. High expression of H3K27me3 is an independent predictor of worse outcome in patients with urothelial carcinoma of bladder treated with radical cystectomy. *Biomed Res Int*. 2013;2013:390482.
15. Liu JY, Zeng QH, Cao PG, et al. SPAG5 promotes proliferation and suppresses apoptosis in bladder urothelial carcinoma by upregulating Wnt3 via activating the AKT/mTOR pathway and predicts poorer survival. *Oncogene*. 2018;37:3937-3952.
16. Liu JY, Zeng QH, Cao PG, et al. RIPK4 promotes bladder urothelial carcinoma cell aggressiveness by upregulating VEGF-A through the NF-kappaB pathway. *Br J Cancer*. 2018;118:1617-1627.
17. Chen J, Du F, Dang Y, et al. FGF19-mediated upregulation of SOX18 promotes hepatocellular carcinoma metastasis by transactivating FGFR4 and FLT4. *Hepatology*. 2020;71:1712-1731.
18. She ZY, Yang WX. SOX family transcription factors involved in diverse cellular events during development. *Eur J Cell Biol*. 2015;94:547-563.
19. Sarkar A, Hochedlinger K. The sox family of transcription factors: versatile regulators of stem and progenitor cell fate. *Cell Stem Cell*. 2013;12:15-30.
20. Huaqi Y, Caipeng Q, Qiang W, et al. The role of SOX18 in bladder cancer and its underlying mechanism in mediating cellular functions. *Life Sci*. 2019;232:116614.

21. Pula B, Kobierzycki C, Solinski D, et al. SOX18 expression predicts response to platinum-based chemotherapy in ovarian cancer. *Anticancer Res.* 2014;34:4029-4037.
22. Jethon A, Pula B, Olbromski M, et al. Prognostic significance of SOX18 expression in non-small cell lung cancer. *Int J Oncol.* 2015;46:123-132.
23. Pula B, Olbromski M, Wojnar A, et al. Impact of SOX18 expression in cancer cells and vessels on the outcome of invasive ductal breast carcinoma. *Cell Oncol (Dordr).* 2013;36:469-483.
24. Hoeth M, Niederleithner H, Hofer-Warbinek R, et al. The transcription factor SOX18 regulates the expression of matrix metalloproteinase 7 and guidance molecules in human endothelial cells. *PLoS One.* 2012;7:e30982.
25. Gao L, Li SH, Tian YX, et al. Role of downregulated miR-133a-3p expression in bladder cancer: a bioinformatics study. *Onco Targets Ther.* 2017;10:3667-3683.
26. Ichimi T, Enokida H, Okuno Y, et al. Identification of novel microRNA targets based on microRNA signatures in bladder cancer. *Int J Cancer.* 2009;125:345-352.
27. Saitoh T, Katoh M. Expression of human SOX18 in normal tissues and tumors. *Int J Mol Med.* 2002;10:339-344.
28. Miao Z, Deng X, Shuai P, et al. Upregulation of SOX18 in colorectal cancer cells promotes proliferation and correlates with colorectal cancer risk. *Onco Targets Ther.* 2018;11:8481-8490.
29. Yin H, Sheng Z, Zhang X, et al. Overexpression of SOX18 promotes prostate cancer progression via the regulation of TCF1, c-Myc, cyclin D1 and MMP-7. *Oncol Rep.* 2017;37:1045-1051.
30. Song T, Xia W, Shao N, et al. Differential miRNA expression profiles in bladder urothelial carcinomas. *Asian Pac J Cancer Prev.* 2010;11:905-911.
31. Zhou Y, Wu D, Tao J, et al. MicroRNA-133 inhibits cell proliferation, migration and invasion by targeting epidermal growth factor receptor and its downstream effector proteins in bladder cancer. *Scand J Urol.* 2013;47:423-432.

SUPPORTING INFORMATION

Additional supporting information may be found online in the Supporting Information section.

How to cite this article: Wang L, Zhang Q, Wu P, et al. SLC12A5 interacts and enhances SOX18 activity to promote bladder urothelial carcinoma progression via upregulating MMP7. *Cancer Sci.* 2020;111:2349–2360. <https://doi.org/10.1111/cas.14502>